Solar Energy Materials & Solar Cells 128 (2014) 427–434

Contents lists available at ScienceDirect

Solar Energy Materials & Solar Cells

journal homepage: www.elsevier.com/locate/solmat

Impact of solar irradiance intensity and temperature on the performance of compensated crystalline silicon solar cells

Chengquan Xiao, Xuegong Yu *, Deren Yang, Duanlin Que

State Key Laboratory of Silicon Materials and Department of Materials Science & Engineering, Zhejiang University, Hangzhou 310027, People's Republic of China

ARTICLE INFO

Article history:
Received 27 August 2013
Received in revised form
3 June 2014
Accepted 5 June 2014

Keywords:
Crystalline silicon solar cell
Dopant compensation
Irradiance intensity
Temperature
Cell efficiency
Performance ratio

ABSTRACT

Low-cost upgraded metallurgical grade silicon (UMG-Si) with inherent boron (B) and phosphorus (P) compensation is a novel material for photovoltaic application. This paper presents the impact of solar irradiance intensity and temperature on the performance of compensated crystalline silicon solar cells. For the same rated output power, compensated crystalline silicon solar cells generate less electricity than the reference silicon solar cells at low irradiance intensity, owing to the strong injection dependence of the carrier lifetime due to high concentration of B–O complexes in compensated silicon. However, at high temperature, compensated crystalline silicon solar cells generate more electricity than the reference silicon solar cells, which mainly originates from the lower temperature-variation of the minority electron mobility in compensated silicon. It suggests that compensated silicon solar cells will be more appropriate for high irradiation application, which often contains high irradiance intensity and high temperature. These results are of great significance for understanding the actual outdoor performance of the solar cells based on the UMG-Si and their application in the photovoltaic (PV) industry.

1. Introduction

Upgraded metallurgical grade silicon (UMG-Si) directly purified by the metallurgical routes has attracted more and more attention in recent years due to the requirement of low cost and therefore has been used to fabricate solar cell in photovoltaic (PV) industry [1,2]. However, the typical characteristic of UMG-Si is the dopant compensation since electrical dopants, such as boron (B) and phosphorus (P), cannot be easily removed via the metallurgical routes [3–6]. Owing to the increased ionized impurity scattering, the dopant compensation might lead to the reduction in both majority and minority carrier mobilities [7,8], but the minority carrier lifetime could get improved benefitting from dopant compensation [9,10]. This counterbalance could result in some improvement in the minority carrier diffusion length [9,10]. Kraiem et al. reported industrial multicrytalline (mc) silicon solar cells with an efficiency of 16.2% and Czochralski (CZ) silicon solar cells with an efficiency of 17.6% using 100% UMG-Si [11]. By adopting a low-temperature dielectric surface passivation on front and rear, Engelhart et al. presented mc UMG-Si solar cells with an efficiency of 18.4% [12]. Recently, Einhaus et al. showed n-type UMG-Si heterojunction (HJ) solar cells with an efficiency of 19.0% [13]. Our previous study shows that compensated silicon solar cells could have a higher open-circuit voltage (V_{oc}), due to a larger net doping concentration (p_0) in the base region, therefore having a comparable efficiency with the conventional ones [8].

It is worth noting that the measurement of the solar cell efficiency (η) is generally performed under the standard test conditions (STC), e.g., an irradiance intensity of 1000 W/m^2 with a spectral distribution conforming to the air mass (AM) 1.5 G spectrum, and a PV device temperature of 25 °C. However, the STC cannot represent the actual outdoor conditions in most regions of the world. The instantaneous power output of a PV module mainly depends on the solar irradiance intensity and operating temperature which significantly vary with the geographical location, climatic conditions, time of day and season [14–17]. Thus, it is necessary to study the performance of solar cells under variable solar irradiance intensities and temperatures in order to be able to provide the accurate prediction of the energy production of PV systems.

In this paper, we have investigated the impact of solar irradiance intensity and temperature on the performance of

* Corresponding author. Fax: +8657187952322.
E-mail address: yuxuegong@zju.edu.cn.(X. Yu)

http://dx.doi.org/10.1016/j.solmat.2014.06.018
0927-0248/

compensated crystalline silicon solar cells. For the reference, the conventional crystalline silicon solar cells are also analyzed in the same measurements. It is found that at low irradiance intensity the performance of compensated crystalline silicon solar cells is relatively worse than that of the reference silicon solar cells, while at high temperature it is relatively better than that of the reference silicon solar cells. These results are of significance for understanding the actual outdoor performance of the solar cells based on the UMG-Si and their application in the PV industry.

2. Experimental procedure

Three 6 in. CZ silicon crystals were grown under the same conditions. One is a conventional B-doped silicon crystal for reference. The other two are compensated silicon crystals grown with electronic grade silicon (EG-Si) voluntarily doped with B and P, labeled as C1 and C2, respectively. All the wafers were sampled from the head part of these crystals. The resistivity ρ of wafers was measured using the four-point-probe (FPP) technique after 650 °C annealing for 30 min in Ar ambient to eliminate the grown-in thermal donors (TDs). The concentrations of B and P in compensated wafers were determined by secondary ion mass spectrometer (SIMS), while the B concentration in the reference wafers was derived from the measured resistivity [18]. The interstitial oxygen concentrations in these wafers were determined by a Fourier transform infrared spectroscope (FTIR, Bruker, IFS 66V/S) with a calibration coefficient of 3.14×10^{17} cm^{-2}. The detailed parameters of these wafers are shown in Table 1. All these wafers were fabricated into solar cells on the same production line at the Trina Solar Company by a standard process, including acid etching, P diffusion, anti-reflection coating deposition, screen-printing and contact firing. Then, these solar cells were cut into small solar cells (840 mm^2 active area) using a high repetition rate Nd:YVO_4 pulsed laser operating at 355 nm. These small solar cells were used for assessing the effect of irradiance intensity and temperature. To stabilize the effect of the metastable B–O complexes under illumination [19–21], all the studied solar cells were first placed under illumination at 323 K for 24 h to ensure that all the B–O complexes were activated and the measured efficiencies of these solar cells were stable. We experimentally checked that there were no more changes in the V_{oc} with additional illumination. So, all these solar cells should achieve complete stabilization. This is also of practical interest since the aim of our study is indeed to compare the performance of the reference and compensated silicon solar cells under real working conditions, which includes full B–O complexes activation.

To investigate the impact of irradiance intensity, current–voltage (I–V) characteristics of the solar cells were measured in the irradiance intensity range of 100–1000 W/m^2, using different neutral filters in the light path of the solar simulator. During the measurement process, the temperature was kept as defined in STC (25 °C). Due to the use of filters, some additional inhomogeneity and a change in spectral composition of irradiance may be induced. Wavelength-dependent absorption graphs of these filters showed the relative deviation of less than 1.5% in wavelength-resolved absorption. This deviation was negligible since it was far below the spectral mismatch of the used light source compared to AM1.5G spectrum. Irradiance intensity was calculated from the ratio of the short-circuit current density J_{sc} of the reference silicon solar cell in the case of applying the filters to the J_{sc} measured at STC, assuming that the J_{sc} was directly proportional to irradiance intensity. It should be mentioned that a possible non-linearity of the J_{sc} with irradiance for compensated silicon solar cells might occur and could be not detected in our study. The values of the series and shunt resistances R_s and R_{sh} were determined by fitting the measured I–V curves using the software tool IVFit [22]. The R_s and R_{sh} were denoted as "apparent" resistances, as a fitting route which calculates from the differential resistance at the V_{oc} and J_{sc} was used. To determine the impact of temperature, the solar cells were placed on a heating chunk under standard illumination condition (AM1.5G; 1000 W/m^2). The temperature was varied from 300 K to 330 K, and the I–V characteristics of the solar cells were measured after the temperature was stabilized.

Table 1
Detailed parameters of the reference and compensated silicon wafers.

Sample	Resistivity (Ω cm)	B concentration (cm^{-3})	P concentration (cm^{-3})	O concentration (cm^{-3})
Reference	2.20	6.3×10^{15}	NA	1.0×10^{18}
C1	0.64	4.1×10^{16}	1.2×10^{16}	1.0×10^{18}
C2	2.84	1.1×10^{17}	9.1×10^{16}	1.0×10^{18}

3. Results and discussion

3.1. Impact of irradiance intensity

Fig. 1 shows the typical I–V and power–voltage (P–V) characteristics of the reference silicon solar cells investigated in this study at 25 °C subjected to different irradiance intensities. It can be seen that with the irradiance intensity decreasing, the V_{oc} decreases slightly while the J_{sc} decreases very sharply. Therefore, the maximum output power decreases with the irradiance intensity decreasing as expected.

Fig. 2 shows the electrical parameters of the reference and compensated silicon solar cells at various irradiance intensities. One can see that the J_{sc} for all these solar cells is generally linear with the irradiance intensity. Therefore, the impact of non-linearity of the J_{sc} with irradiance in our study is very small for compensated silicon solar cells, as can be seen from Fig. 2a. The V_{oc} is logarithmically dependent on the irradiance intensity. Due to the logarithmic irradiance scale, the apparent linear relationship between the V_{oc} and irradiance intensity can be seen for all the solar cells (Fig. 2b). The fill factor FF presents an initial increase and subsequent decrease with the irradiance intensity decreasing (Fig. 2c). The increase in FF upon lowering the irradiance intensity could be explained by the series resistance effects, as a lower current leads to quadratically lower Joule losses. It should be mentioned that the Joule losses are linearly dependent on the series resistance, but they are quadratically dependent on the current. So, the current has a bigger impact on the Joule losses than the series resistance. Upon lowering the intensity, the current decreases very sharply, which could counterbalance the effect of

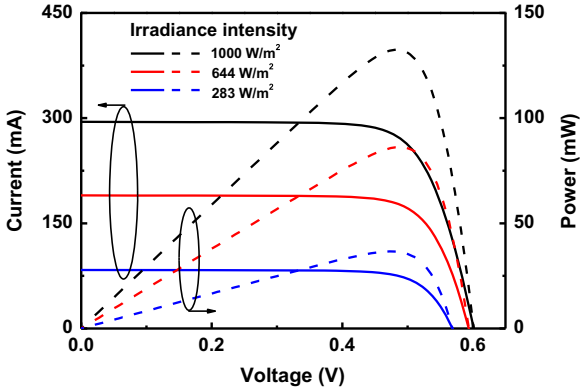

Fig. 1. Current–voltage (I–V) and power–voltage (P–V) characteristics of solar cells at 25 °C under various irradiance intensities.

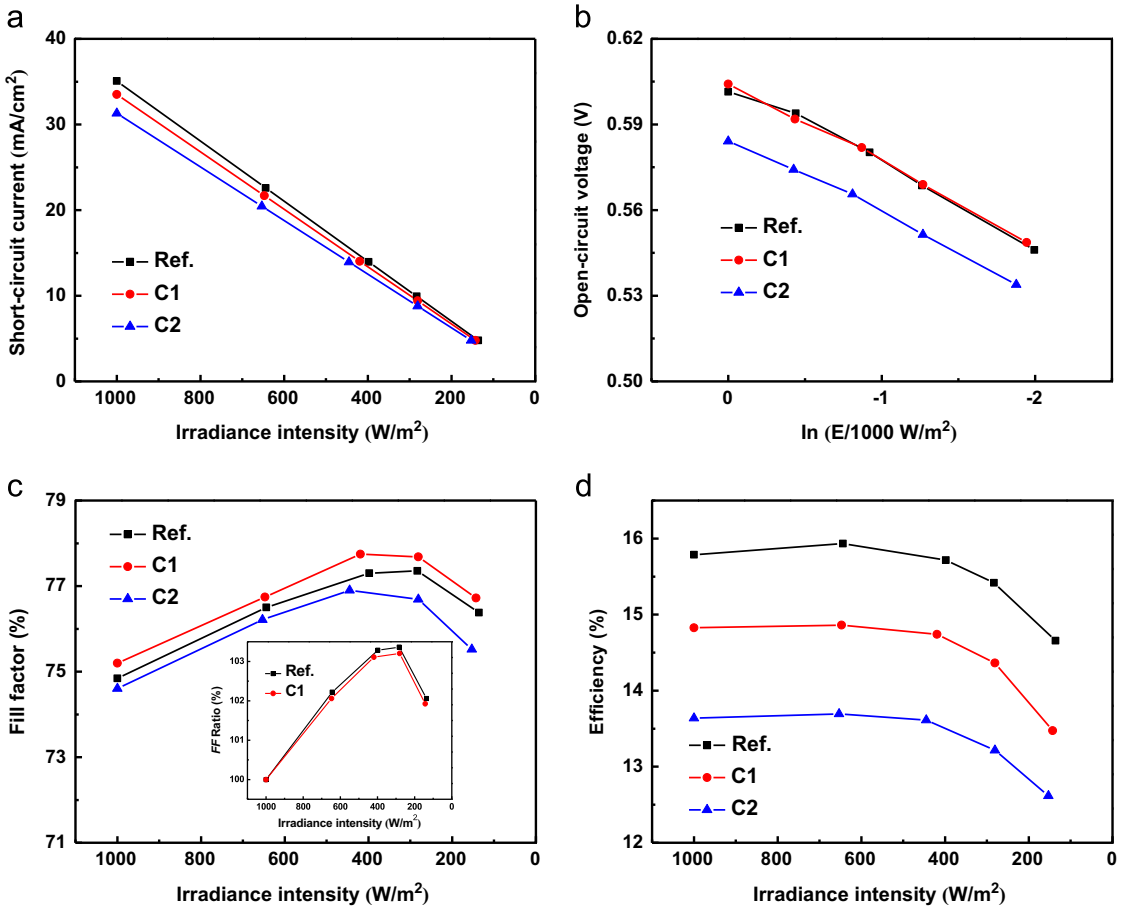

Fig. 2. Electrical parameters of the reference and compensated silicon solar cells under different irradiance intensities. The inset graph in (c) is the fill factor ratio (*FF*) ratio.

increased series resistance and finally result in reduced Joule losses. However, the reduction in *FF* under very low irradiance intensity should mainly originate from the shunt resistivity effects, as the saturation current J_o has a greater influence on the *FF* [23]. Since the η of the solar cells is dependent on the product of J_{sc}, V_{oc} and *FF*, the η of all the solar cells also present an initial increase and subsequent decrease with the irradiance intensity decreasing (Fig. 2d). Considering that the J_{sc} is linearly dependent on the irradiance intensity, the variation in the η should mainly originate from the variation of the product of V_{oc} and *FF*.

Fig. 3 presents the performance ratio (PR) for the reference and compensated silicon solar cells at various irradiance intensities. Here, PR is defined as $\eta(G)/\eta(G=1000)$, where $\eta(G)$ and $\eta(G=1000)$ are the cell efficiency under the actual and standard illumination conditions, respectively. It should be mentioned that the data of performance ratios for each kind of solar cells are from the statistical average of 5 cells in our study. Moreover, the values of performance ratios are almost the same for the same kind of solar cells. As shown in Fig. 3, the performance of p-type compensated silicon solar cells is relatively worse than that of the reference silicon solar cells at low irradiance intensity. For instance, the value of PR for the reference silicon solar cells at 136 W/m^2 is 92.8%, while 90.9% for the C2 solar cells. It means that for the same rated output power, compensated silicon solar cells will generate less electricity than the reference silicon solar cells at low irradiance intensity. This result is consistent with the outdoor monitoring of PV modules based on UMG-Si and classical silicon feedstock, which was recently reported by Sánchez et al. [24]. The relatively worse performance of the solar cells at low irradiance intensity might originate from the low shunt resistance R_{sh}. However, the values of R_{sh} for the reference and compensated

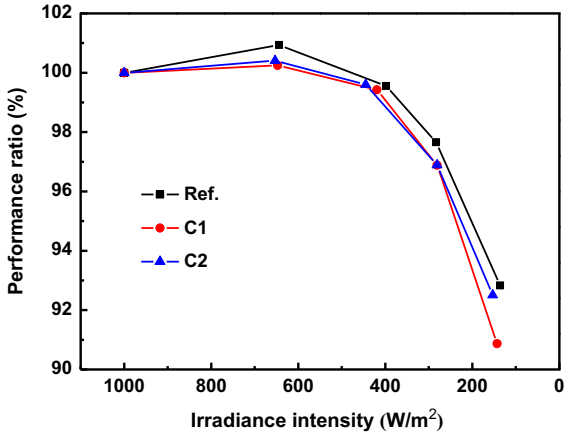

Fig. 3. Performance ratio (PR) for the reference and compensated silicon solar cells under different irradiance intensities.

silicon solar cells are mostly the same, i.e., R_{sh}=0.4–0.5 kΩ cm^2 (Fig. 4b). Gong et al. have demonstrated that the performance of p-type silicon solar cells at low irradiance intensity can be influenced by the injection-level effects [25]. As mentioned above, all the studied cells underwent a complete light-induced degradation. We found that only compensated silicon solar cells are sensitive to the light-induced degradation effect, due to the generation of high concentration of B–O complexes [26]. Therefore, the carrier lifetime in compensated silicon solar cells is mainly limited by high concentration of B–O complexes, while that in the reference silicon is mainly limited by low concentration of B–O complexes. It is well known that the B–O complexes

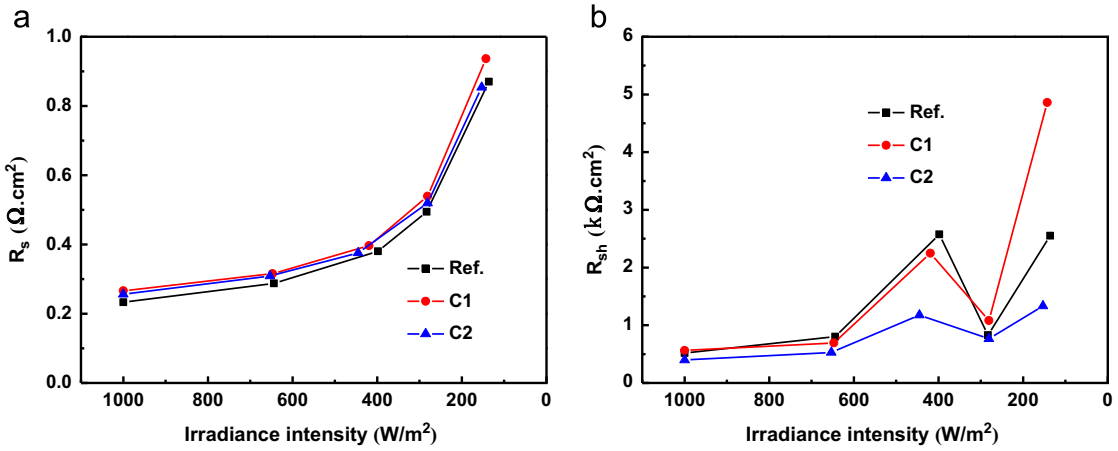

Fig. 4. Series resistance (R_s) and shunt resistance (R_{sh}) for the reference and compensated silicon solar cells under different irradiance intensities.

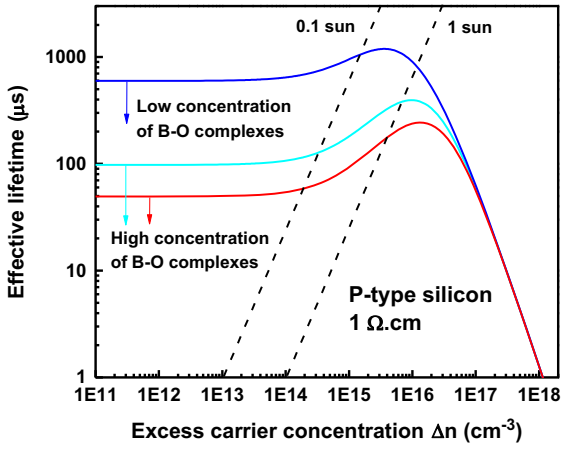

Fig. 5. Carrier lifetime in silicon dominated by different concentrations of B–O complexes as a function of the excess carrier concentration.

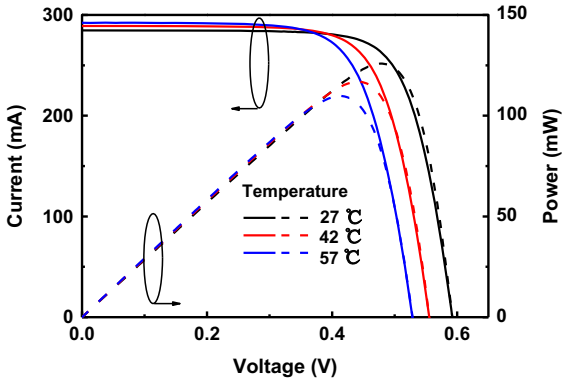

Fig. 6. Current–voltage (I–V) and power–voltage (P–V) characteristics of solar cells under the irradiance intensity of 1000 W/m^2 at different temperatures.

introduce an energy level at E_c–0.41 eV in silicon band gap, with an electron/hole capture cross-section ratio (σ_n/σ_p) being approximated to 10 [27]. However, the detailed σ_n and σ_p of B–O complexes are still unclear. For the purpose of illustrating the principal effects, the σ_n and σ_p of B–O complexes are assumed to be 1×10^{-14} cm^2 and 1×10^{-15} cm^2, respectively. Therefore, the carrier lifetime as a function of the excess carrier concentration can be simulated on the basis of Shockley–Read–Hall (SRH) theory [28].

Fig. 5 shows the simulated carrier lifetime in silicon dominated by different concentrations of B–O complexes as a function of the excess carrier concentration when irradiance intensity decreases from 1 sun (1000 W/m^2) to 0.1 sun (100 W/m^2). The intrinsic recombination comprised of Auger and radiative recombination has also been taken into account in our simulation [29]. As shown in Fig. 5, one can observe that with the irradiance intensity decreasing, the carrier lifetime dominated by low concentration of B–O complexes is hardly affected, while the carrier lifetime dominated by high concentration of B–O complexes decreases sharply. Therefore, the relatively worse performance of compensated silicon solar cells at low irradiance intensity should be mainly attributed to the strong injection dependence of the carrier lifetime on high concentration of B–O complexes. Note, the values of the V_{oc} in the C1 solar cells are almost the same as those in the reference silicon solar cells at different irradiance intensities (Fig. 2b). Therefore, the difference of the variation in the η between the C1 and reference silicon solar cells mainly originates from the difference of the variation of the *FF*, which can be seen from the inset graph of Fig. 2c. So, the underlying reason for the relatively worse performance of compensated silicon solar cells at low irradiance intensity is that the strong injection-dependent characteristics of the carrier lifetime limited by the B–O complexes cause a larger reduction in *FF*, which is consistent with the results reported by Schmidt et al. [30].

It should be mentioned that the carrier lifetime dominated by B–O complexes could get improved under high irradiation conditions, resulting from the nature of the deep level defect (Fig. 5c). Recently, Søiland et al. reported that compared to the conventional silicon solar cells, compensated silicon solar cells show an improved performance under high irradiation conditions [31].

3.2. Impact of temperature

Fig. 6 shows the typical I–V and P–V characteristics of the reference silicon solar cells investigated in this study under the illumination intensity of 1000 W/m^2 at different temperatures. It can be seen that with the temperature increasing, the J_{sc} increases slightly and the V_{oc} decreases strongly. The slight increase in the J_{sc} originates from the narrowing of the band gap along with the increase in the number of phonons and density of states in the conduction and valence bands, while the strong decrease in the V_{oc} is mainly linked to the increase of the leakage current [32]. As a result, the maximum output power decreases with the temperature increasing.

Fig. 7 presents the PR for the reference and compensated silicon solar cells at various temperatures. At high temperature, the performance of compensated silicon solar cells is relatively better than that of the reference silicon solar cells. For example, the value of PR for the reference silicon solar cells at 57 °C is 86.5%, while 87.4% for the C2 solar cells. It means that for the same rated output power, compensated silicon solar cells will generate more electricity than the reference silicon solar cells at high temperature. It suggests that compensated silicon might be more acceptable for the future of PV industry since the temperature of PV modules is generally higher than 25 °C under real working conditions.

By plotting the electrical parameters of the reference and compensated silicon solar cells as a function of temperature, it is found that the electrical parameters of all the solar cells vary linearly with the temperature. The slopes of the linear functions

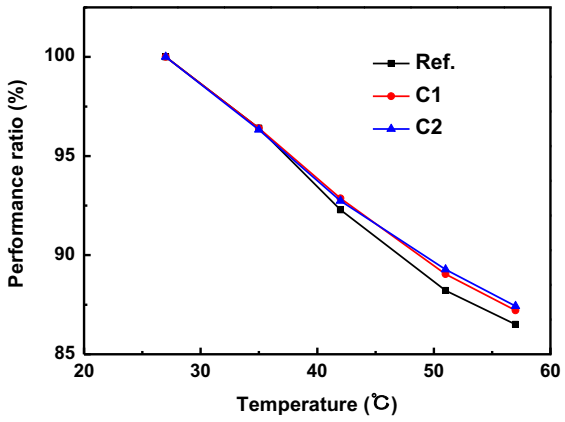

Fig. 7. Performance ratio (PR) for the reference and compensated silicon solar cells at different temperatures.

(pre-factors dJ_{sc}/dT, dV_{oc}/dT, dFF/dT and $d\eta/dT$) are extracted from the experimental T-variations of the J_{sc}, V_{oc}, FF and η, respectively, see Fig. 8. It can be seen that the dV_{oc}/dT and dFF/dT values of the reference and compensated silicon solar cells are almost same, while the dJ_{sc}/dT values of compensated silicon solar cells are significantly higher than those of the reference silicon solar cells. Therefore, owing to the strong increase of the J_{sc} with the temperature increasing, the $d\eta/dT$ values of compensated silicon solar cells are significantly lower in absolute than those of the reference silicon solar cells. For instance, the dJ_{sc}/dT and $d\eta/dT$ values of the reference silicon solar cells are 2.05×10^{-2} mA/cm^2/K^{-1} and -7.52% K^{-1}, respectively, while the dJ_{sc}/dT and $d\eta/dT$ values of the C2 silicon solar cells are 3.58×10^{-2} mA/cm^2/K and -5.69% K^{-1}, respectively.

For a standard industrial solar cell, the J_{sc} can be strongly influenced by the minority carrier diffusion length, which depends on the product of the minority electron mobility and carrier lifetime [10]. Considering that the temperature has the same influence on the carrier lifetimes in compensated and reference silicon, since they are mainly dominated by the same kind of defect centers "B–O complexes". Therefore, it is suspected that the difference of dJ_{sc}/dT between compensated and reference silicon solar cells might originate from the variation of the minority electron mobility with the temperature. Here, Klaassen's model was used in our study to describe the relationship between the minority electron mobility and temperature [33,34]. In this model, lattice scattering, ionized acceptor and donor impurities scattering and electron–hole scattering are considered. The total minority electron mobility μ_e can be given by the sum of these terms:

$$\frac{1}{\mu_e}=\frac{1}{\mu_{e,L}}+\frac{1}{\mu_{e,A}}+\frac{1}{\mu_{e,D}}+\frac{1}{\mu_{e,h}} \quad (1)$$

where $\mu_{e,L}$, $\mu_{e,A}$, $\mu_{e,D}$ and $\mu_{e,h}$ are the minority electron mobilities limited by lattice, acceptor, donor and hole, respectively.

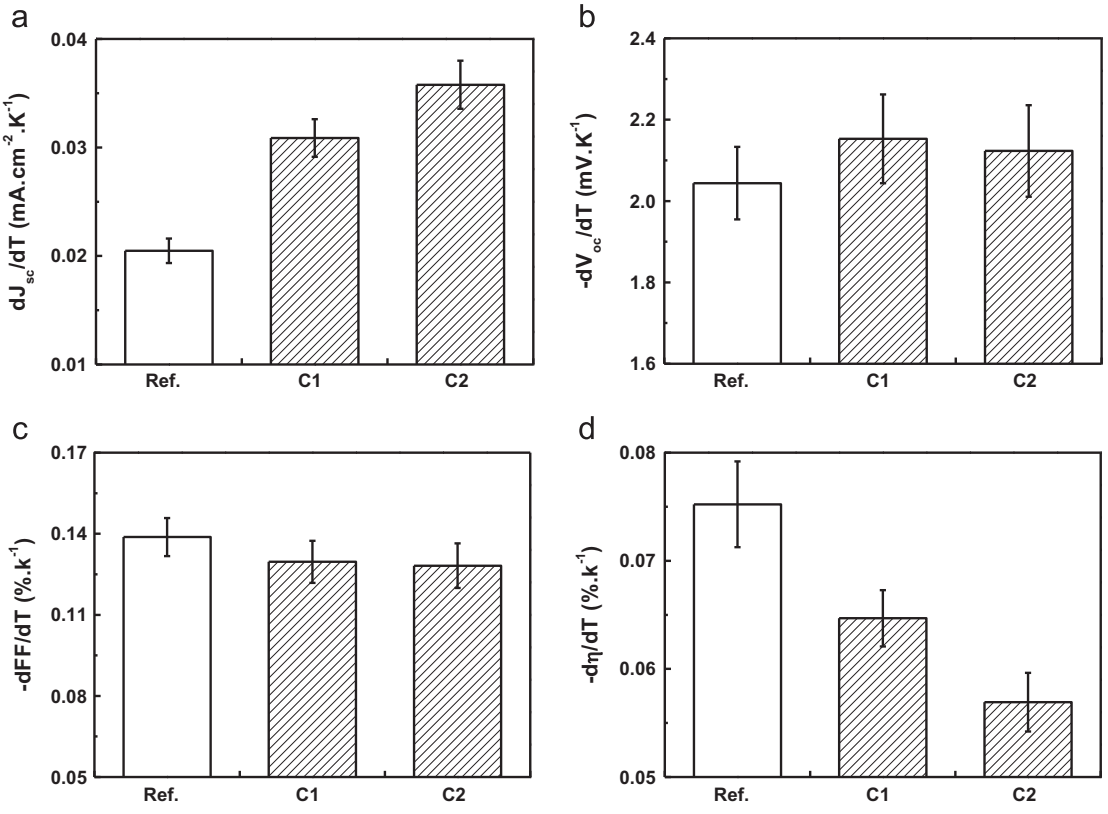

Fig. 8. (a) Pre-factors dJ_{sc}/dT, (b) pre-factors dV_{oc}/dT, (c) prefactors dFF/dT and (d) pre-factors $d\eta/dT$ for the reference and compensated silicon solar cells.

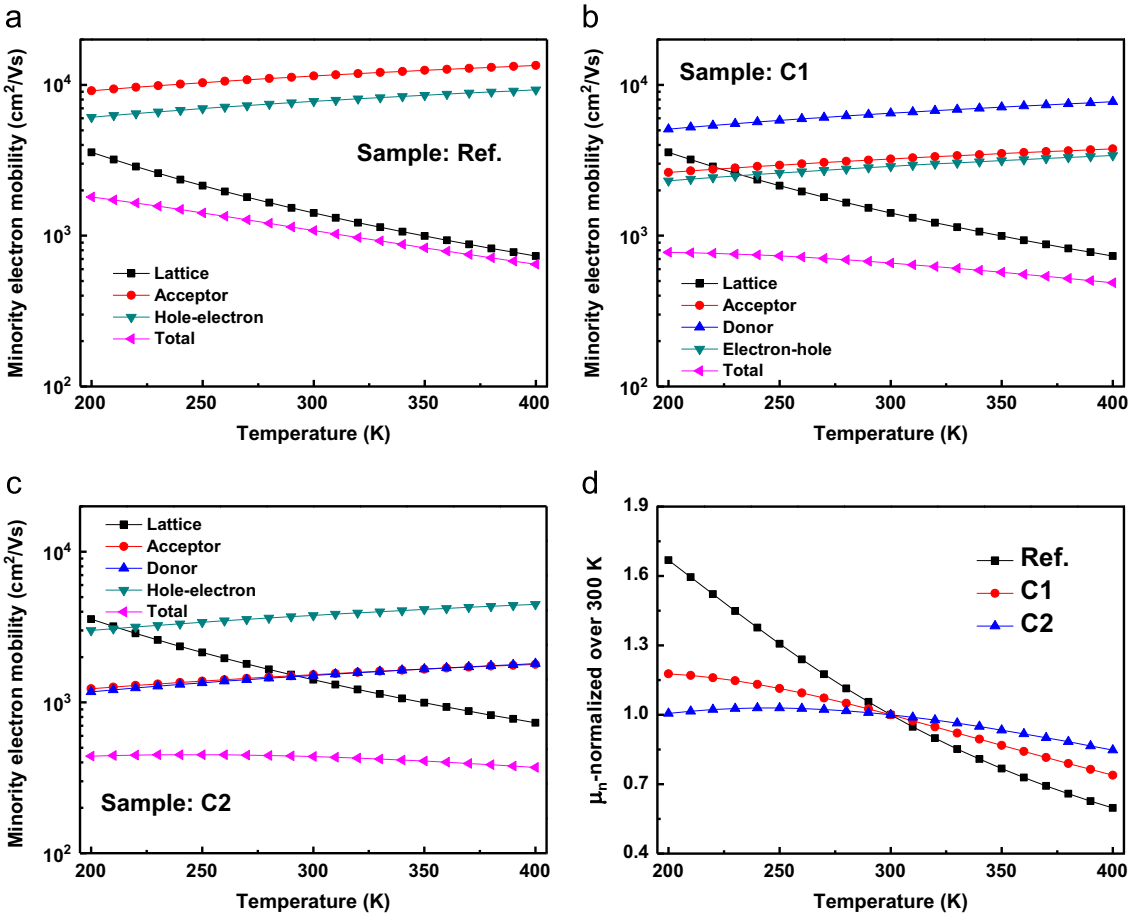

Fig. 9. Temperature dependence of the minority electron mobility in the (a) reference, (b) C1 and (c) C2 silicon based on Klaassen's model. (d) Normalized values, normalization over 300 K for three samples (ratio of the value at the given temperature over the value at 300 K).

Fig. 9 shows the temperature dependence of the minority electron mobility in the reference, C1 and C2 silicon. It can be seen that with the temperature increasing, the $\mu_{e,L}$ decreases very sharply, while the $\mu_{e,A}$, $\mu_{e,D}$ and $\mu_{e,h}$ slightly increase. The reason is that lattice scattering affects the minority electron mobility by means of the interaction with phonons whose number increases sharply with the temperature, while ionized impurity scattering and electron–hole scattering affect the minority electron mobility by means of Coulombic interaction with fixed (B^- or P^+) and moving (hole) charges, respectively. With the temperature increasing, the number of fixed and moving charges keeps almost constant in the studied temperature range, while the velocities of the minority electrons become large and therefore the time of the minority electrons passing the fixed or moving charges becomes shorter. In other words, with the temperature increasing, the reduced collision cross-section between the minority electrons and charges weakens the scatterings between the minority electrons and charges [34]. Therefore, the $\mu_{e,A}$, $\mu_{e,D}$ and $\mu_{e,h}$ increase with the temperature increasing. Meanwhile, owing to the greater dopant concentration and the generally stronger majority carrier concentration in compensated silicon, the ionized impurity scattering and electron–hole scattering have a much stronger influence on the total minority electron mobility. The dominant scattering mechanism in the reference silicon is only lattice scattering, while the dominant scattering mechanisms in compensated silicon are both lattice scattering and ionized impurity scattering (Fig. 9(a–c)). As a result, as the temperature rises, the increasing scattering on phonons is counterbalanced by a decreasing scattering on ionized impurities, resulting in an overall temperature-independent mobility. As shown in Fig. 9(d), the variation of the minority electron mobility in compensated silicon with temperature is significantly lower than that in the reference silicon, which is consistent with the lower temperature-variation of the Hall mobility in compensated mc-Si reported by Mondanese et al. [35]. Therefore, the higher values of dJ_{sc}/dT for compensated silicon solar cells should be mainly ascribed to the low variation of the minority electron mobility with the temperature increasing. Notably, the dJ_{sc}/dT of the C2 silicon solar cells shows the highest value, owing to the lowest variation of the minority electron mobility with temperature. It should be mentioned that Klaassen's model may overestimate the value of the minority carrier mobility in compensated silicon [36,37]. However, in the case of a low compensation level (lower than 10), the minority carrier mobility is consistent with the predicted values based on Klaassen's model [37]. In this study, the compensation levels for the C1 and C2 wafers are 2 and 9, respectively. Therefore, it is reasonable to use Klaassen's model in our study. In addition, our previous work also shows that the measured minority carrier mobilities in compensated silicon at room temperature are basically in good agreement with the predicted values [8].

Tanay et al. presented the difference of the T-coefficients between the conventional and UMG-Si solar cells [38]. The value of temperature-coefficient was found to be $-7.0\times10^{-2}\%\,K^{-1}$ for the EG-Si cell, while it was $-4.5\times10^{-2}\%\,K^{-1}$ for the SoG-Si cell. However, our study not only shows the difference of the T-coefficients between the conventional and compensated silicon solar cells, but also shows the difference of the T-coefficients between compensated silicon solar cells with different compensation

levels. The value of temperature-coefficient is $-6.5\times10^{-2}\%\,K^{-1}$ for the lightly-compensated silicon solar cell, while it is $-5.7\times10^{-2}\%\,K^{-1}$ for the highly-compensated silicon solar cell. Our theoretical calculations show that the variation of the minority electron mobility in the C2 wafer with temperature is significantly lower than those in the reference and C1 wafers. Therefore, our results further confirm that the lower temperature-coefficient of compensated silicon solar cells originates from the lower temperature-variation of the minority electron mobility. With the temperature increasing, the narrowing of the band gap along with the increase in the number of phonons and density of states in the CB and the VB could cause the increase of the number of absorbed phonons and therefore result in an improvement in J_{sc} for all the solar cells, which is compensation–independent. However, the increased temperature will generally cause the different reduction of the minority electron mobility in compensated and reference silicon, which is compensation-dependent and therefore results in the difference between temperature coefficients for compensated or reference cells.

4. Conclusions

In summary, we have investigated the impact of solar irradiance intensity and temperature on the performance of compensated crystalline silicon solar cells. At low irradiance intensity, compensated silicon solar cells show relatively worse performance than the reference silicon solar cells, which has been explained by the strong injection dependence of the carrier lifetime due to the existence of high concentration of B–O complexes in compensated silicon. At high temperature, compensated silicon solar cells show relatively better performance than the reference silicon solar cells, which is associated to the lower variation of the minority electron mobility with temperature. These results are of great significance for understanding the actual outdoor performance of UMG-Si solar cells and their application in PV industry.

Acknowledgments

This work is supported by National Natural Science Foundation of China (no. 61274057), National Key Technology R&D Program (2011BAE03B13), and Innovation Team Project of Zhejiang Province (2009R50005).

References

[1] S. De Wolf, J. Szlufcik, Y. Delannoy, I. Perichaud, C. Habler, R. Einhaus, Solar cells from upgraded metallurgical grade (UMG) and plasma-purified UMG multicrystalline silicon substrates, Sol. Energy Mater. Sol. Cells 72 (2002) 49–58.
[2] A.F.B. Braga, S.P. Moreira, P.R. Zampieri, J.M.G. Bacchin, P.R. Mei, New processes for the production of solar-grade polycrystalline silicon: a review, Solor Energy Mater. Sol. Cells 92 (2007) 418–424.
[3] N. Yuge, H. Baba, Y. Sakaguchi, K. Nishikawa, H. Terashima, F. Aratani, Purification of metallurgical silicon up to solar grade, Solor Energy Mater. Sol. Cells 34 (1994) 243–250.
[4] C. Alemany, C. Trassy, B. Pateyron, K.-I. Li, Y. Delannoy, Refining of metallurgical-grade silicon by inductive plasma, Solor Energy Mater. Sol. Cells 72 (2002) 41–48.
[5] J.C.S. Pires, J. Otubo, A.F.B. Braga, P.R. Mei, The purification of metallurgical grade silicon by electron beam melting, J. Mater. Process. Technol. 169 (2005) 16–20.
[6] G. Flamant, V. Kurtcuoglu, J. Murray, A. Steinfeld, Purification of metallurgical grade silicon by a solar process, Solor Energy Mater. Sol. Cells 90 (2006) 2099–2106.
[7] F.E. Rougieux, D. Macdonald, A. Cuevas, S. Ruffell, J. Schmidt, B. Lim, A.P. Knights, Electron and hole mobility reduction and hall factor in phosphorus-compensated p-type silicon, J. Appl. Phys. 108 (2010) (013706-1-013706-5).
[8] C.Q. Xiao, D.R. Yang, X.G. Yu, P. Wang, P. Chen, D.L. Que, Effect of dopant compensation on the performance of Czochralski silicon solar cells, Sol. Energy Mater. Sol. Cells 101 (2012) 102–106.
[9] S. Dubois, N. Enjalbert, J.P. Garandet, Effect of the compensation level on the carrier lifetime of crystalline silicon, Appl. Phys. Lett. 93 (2008) (032114-1-032114-3).
[10] C.Q. Xiao, D.R. Yang, X.G. Yu, X. Gu, D.L. Que, Influence of the compensation level on the performance of p-type crystalline silicon solar cells: theoretical calculations and experimental study, Sol. Energy Mater. Sol. Cells 107 (2012) 263–271.
[11] J. Kraiem, B. Drevet, F. Cocco, N. Enjalbert, S. Dubois, D. Camel, D. Grosset-Bourbange, D. Pelletier, T. Margaria, R. Einhaus, High performance solar cells made from 100% UMG silicon obtained via the PHOTOSIL process, in: Proceedings of the 35th IEEE Photovoltaic Specialists Conference, Honolulu, June 2010, pp. 1427–1431.
[12] P. Engelhart, J. Wendt, A. Schulze, C. Klenke, A. Mohr, K. Petter, F. Stenzel, S. Hörnlein, M. Kauert, M. Junghänel, B. Barkenfelt, S. Schmidt, D. Rychtarik, M. Fischer, J.W. Müller, P. Wawer, R&D pilot line production of multi-crystalline Si solar cells exceeding cell efficiencies of 18%, Energy Procedia 8 (2011) 313–317.
[13] R. Einhaus, J. Kraiem, J. Degoulange, O. Nichiporuk, M. Forster, P. Papet, Y. Andrault, D. Grosset-Bourbange, F. Cocco, 19% efficiency heterojunction solar cells on Cz wafers from non-blended upgraded metallurgical silicon, in: Proceedings of the 38th IEEE Photovoltaic Specialists Conference, Austin, June 2012, pp. 3234–3237.
[14] T. Minemoto, S. Nagae, H. Takakura, Impact of spectral irradiance distribution and temperature on the outdoor performance of amorphous Si photovoltaic modules, Sol. Energy Mater. Sol. Cells 91 (2007) 919–923.
[15] T. Ishii, K. Otani, T. Takashima, Effects of solar spectrum and module temperature on outdoor performance of photovoltaic modules in round-robin measurements in Japan, Prog. Photovoltaics Res. Appl. 19 (2011) 141–148.
[16] T. Ishii, K. Otani, T. Takashima, S. Kawai, Estimation of the maximum power temperature coefficients of PV modules at different time scales, Sol. Energy Mater. Sol. Cells 95 (2011) 386–389.
[17] N.H. Reich, B. Mueller, A. Armbruster, W. Sark, K. Kiefer, C. Reise, Performance ratio revisited: is PR $>90\%$ realistic, Prog. Photovoltaics Res. Appl. 20 (2012) 717–726.
[18] Standard Practice for Conversion Between Resistivity and Dopant Density for Boron-doped, Phosphorus-doped and Arsenic-doped Silicon. Designation: ASTM-F723, 1999.
[19] V. Meemongkolkiat, K. Nakayashiki, A. Rohatgi, G. Crabtree, J. Nickerson, T.L. Jester, Resistivity and lifetime variation along commercially grown Ga- and B-doped Czochralski Si ingots and its effect on light-induced degradation and performance of solar cells, Prog. Photovoltaics Res. Appl. 14 (2006) 125–134.
[20] B. Lim, S. Hermann, K. Bothe, J. Schmidt, R. Brendel, Solar cells on low-resistivity boron-doped Czochralski-grown silicon with stabilized efficiencies of 20%, Appl. Phys. Lett. 93 (2008) (162102-1-162102-3).
[21] P. Wang, X.G. Yu, P. Chen, X.Q. Li, D.R. Yang, X. Chen, Z.F. Huang, Germanium-doped Czochralski silicon for photovoltaic applications, Sol. Energy Mater. Sol. Cells 95 (2011) 2466–2470.
[22] T. Burgers, IVFIT Program, Downloadable at ⟨http://www.ecn.nl/en/zon/products-services/i-v-curve-fitting-program-ivfit/⟩.
[23] G.E. Bunea, K.E. Wilson, Y. Meydbray, M.P. Campbell, D.M.D. Ceuster, Low light performance of mono-crystalline silicon solar cells, in: Proceedings of the 2006 IEEE Fourth World Conference on Photovoltaic Energy Conversion, Waikoloa, May 2006, pp. 1312–1314.
[24] E. Sánchez, J. Torreblanca, T. Carballo, V. Parra, J. Bullon, J.M. Miguez, J. Gutierrez, J. Garcia, I. Guerrero, R. Ordas, J. Izard, Outdoor monitoring of the energy yield and electrical parameters of standard polysilicon based and new umg-Si PV modules, Energy Procedia 8 (2011) 503–508.
[25] C. Gong, N. Posthuma, F. Dross, E.V. Kershaver, F. Giovanni, G. Beaucarne, J. Poortmans, Comparison of n- and p-type high efficiency silicon solar cell performance under low illumination conditions, in: Proceedings of the 23rd European Photovoltaic Solar Energy Conference and Exhibition, Valencia, Spain, 2008, pp. 1360–1363.
[26] C.Q. Xiao, X.G. Yu, D.R. Yang, D.L. Que, Study on permanent deactivation of the light-induced degradation in p-type compensated crystalline silicon solar cells, Sol. Energy Mater. Sol. Cells 117 (2013) 29–33.
[27] S. Rein, S.W. Glunz, Electronic properties of the metastable defect in boron-doped Czochralski silicon: unambiguous determination by advanced lifetime spectroscopy, Appl. Phys. Lett. 82 (2003) 1054–1056.
[28] W. Shockley, W.T. Read, Statistics of the recombinations of holes and electrons, Phys. Rev. 87 (1952) 835–842.
[29] A. Richter, S.W. Glunz, F. Werner, J. Schmidt, A. Cuevas, Improved quantitative description of Auger recombination in crystalline silicon, Phys. Rev. B: Condens. Matter 86 (2012) (165202-1-165202-14).
[30] J. Schmidt, A. Cuevas, S. Rein, S.W. Glunz, Impact of light-induced recombination centres on the current–voltage characteristic of Czochralski silicon solar cells, Prog. Photovoltaics Res. Appl. 9 (2001) 249–255.
[31] A. Søiland, J.O. Odden, B. Sandberg, K. Friestad, J. Håkedal, E. Enebakk, S. Braathen, Solar silicon from a metallurgical route by Elkem solar—a viable alternative to virgin polysilicon, in: Proceedings of the Sixth International Workshop on Crystalline Silicon Solar Cells, Aix-les-bains, France, 2012.
[32] J.D. Arora, P.C. Mathur, Behavior of diffused junction silicon solar cells in the temperature range 77–500 K, J. Appl. Phys. 52 (1980) 3646–3650.
[33] D.B.M. Klaassen, A unified mobility model for device calculation-I. Model equations for and concentration dependence, Solid-State Electron. 35 (1992) 953–959.

[34] D.B.M. Klaassen, A unified mobility model for device calculation-II. Temperature dependence of carrier mobility and lifetime, Solid-State Electron. 35 (1992) 961–967.
[35] C. Modanese, M. Acciarri, S. Binetti, A. Søiland, M.D. Sabatino, L. Arnberg, Temperature-dependent hall-effect measurements of p-type multicrystalline compensated solar grade silicon, Prog. Photovoltaics Res. Appl. (2012), http://dx.doi.org/10.1002/pip.2223.
[36] B. Lim, F. Rougieux, D. Macdonald, K. Bothe, J. Schmidt, Generation and annihilation of boron-oxygen-related recombination centers in compensated p- and n-type silicon, J. Appl. Phys. 108 (2010) (103722-1-103722-9).
[37] M. Forster, F. Rougieux, A. Cuevas, B. Dehestru, A. Thomas, E. Fourmond, M. Lemiti, Incomplete ionization and carrier mobility in compensated p-type and n-type silicon, IEEE J. Photovoltaics 3 (2013) 108–113.
[38] F. Tanay, S. Dubois, N. Enjalbert, J. Veirman, Low temperature-coefficient for solar cells processed from solar-grade silicon purified by metallurgical route, Prog. Photovoltaics Res. Appl. 19 (2011) 966–972.